Sensor and Simulation Notes

Note 326

10 April 1991

CANONICAL EXAMPLES OF HIGH-POWER MICROWAVE (HPM) RADIATION SYSTEMS FOR THE CASE OF ONE FEEDING WAVEGUIDE

by

D. V. Giri, Ph.D.

Pro-Tech, 3708 Mt. Diablo Boulevard, #110, Lafayette, CA 94549-3610

Abstract

In an earlier note on this subject [1], we had addressed some preliminary considerations for HPM radiation systems and concluded that a single or a dual reflector antenna system is well suited for broadcasting a directive HPM beam. With the objective of maximizing the field at a distance, some canonical example systems are worked out here, based on certain assumptions of power levels, frequency and nature of the output from HPM sources. Specifically, we consider average power levels of 3 GW and 10 GW at 1 GHz, and 1 GW and 3 GW at 3 GHz, delivered by suitable sources, with pulse widths of 100 ns and 1 μs in each case. The radiating aperture area is chosen to have values of 20 m^2, 40 m^2 and 100 m^2 from practical considerations. Both single and dual reflector antenna systems are considered, with a single feed horn in each case. The subject of an array of feed horns illuminating the reflector, is not treated here and will be the topic of a future note.

PREFACE

This work was performed by Pro-Tech for the Department of Electrical Engineering, University of California at Los Angeles (UCLA), and was sponsored by the U.S. Army. The author is thankful to Professor Y. Rahmat-Samii of UCLA for his encouragement and support, and to Dr. Carl Baum of Phillips Laboratory, Kirtland AFM, NM for valuable discussions.

Contents

1. Introduction

The objective of this note is to consider some canonical radiating systems, in as much detail as feasible, in order to broadcast directive HPM radiation. A previous note [1] discussed some preliminary considerations for HPM radiating systems, by investigating the applicability of several classical radiating systems. It was concluded that reflector antennas in general and an offset Cassegrain system in particular are well suited for generating directive HPM beams. It is observed that the power is extracted from the source in N number of evacuated rectangular waveguides (say). Here N can be 1 or more depending on the source and power level etc. We have found it instructive to assume N to be 1 to start with, and investigate canonical examples of the HPM radiation systems. In other words, what level of far fields can one produce given that all of the HPM power is extracted from a suitable source in a single evacuated rectangular waveguide? Future notes will consider values of $N > 1$, requiring a feed array. At this stage the case of $N = 1$ is of interest and as we see in later sections, quite instructive.

Having chosen the case of a single waveguide carrying the microwave power out of a suitable source (Xatron), one needs to make certain assumptions about the frequencies, power levels and pulse widths, before considering the feed and radiation system examples. These assumptions are discussed in the next section. It is noted however, whatever the source may be, a vacuum flange can be treated as an universal interface where the "source" terminates and the feed elements begin. To the left of this vacuum flange is the source and to its right are the elements of the feed system. Figure 1 shows a block schematic of the radiating system from the source to a single

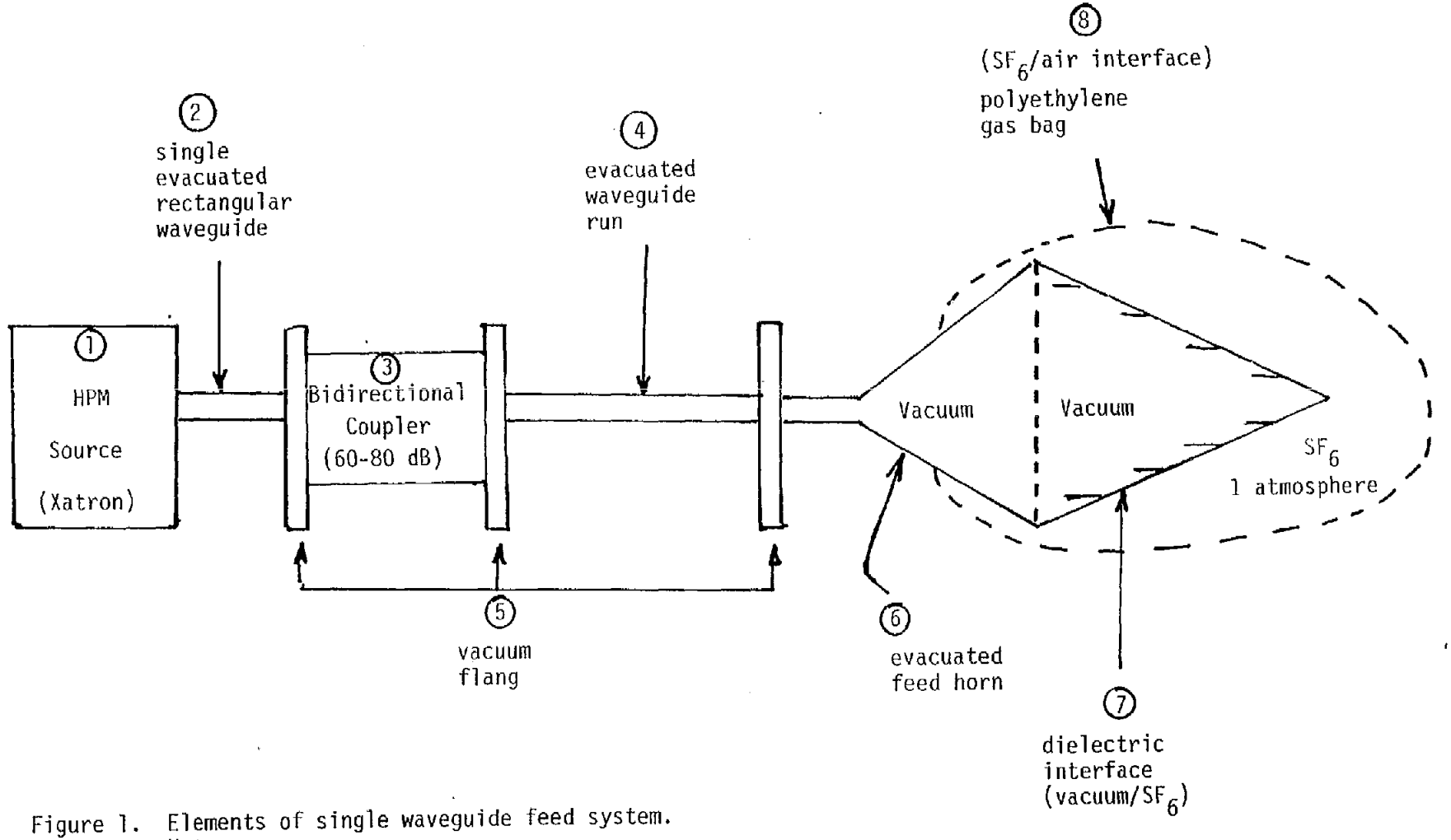

Figure 1. Elements of single waveguide feed system.

Notes

1. any suitable HPM source
2. evacuated rectangular waveguide with dominant mode propagation
3. magnetic wall coupler (60 to 80 dB)
4. evacuated wavegude run to the feed horn
5. standard vacuum flanges
6. evacuated feed horn (e.g., pyramidal) with rounded metallic edges
7. vacuum to SF_6 dielectric interface with suitable metal slats
8. gas bag to transition from SF_6 to air outside that may contain parts of the reflectors in it

feed horn. With reference to this figure, we see an HPM source with a single rectangular waveguide power extraction. The leftmost vacuum flange is the universal interface between the source and the feed system. Following this is a bidirectional coupler (60-dB) again ending in a vacuum flange. We then have a section of a waveguide run to a vacuum flange to which the feed horn is connected. The feed horn, which could be pyramidal is also evacuated and a dielectric interface between vacuum and 1 atmosphere SF_6 is present at the horn aperture. A polyethylene container may be used for holding the SF_6 gas and the container is then an interface between the SF_6 gas and the outside air. All of these elements going from the source to the feed horn are schematically shown in figure 1 and described later in greater detail for a particular set of assumptions about the prescribed HPM source. The various interfaces starting from hard vacuum to outside air, via 1 atmosphere SF_6 gas are so designed that the peak electric field anywhere in the outside air medium does not exceed 1 MV/m. The field anywhere in the SF_6 medium is designed not to exceed 3 MV/m. These values have adequate safety margins.

It is noted that we have not so far shown the reflector antenna system illuminated by the feed horn of figure 1. Two possibilities [2] are; (1) an offset parabolic reflector and (2) dual offset reflector system, as illustrated in figures 2 and 3. In both cases, the aperture of the main reflector is shown to be circular as an example. Practical consideration in specific situations will influence the size and shape of the main reflector. Furthermore, the extant of the SF_6 gas bag and its relationship to the reflectors (main and/or sub reflector) is also governed by the peak field levels in this region, as we see in later sections.

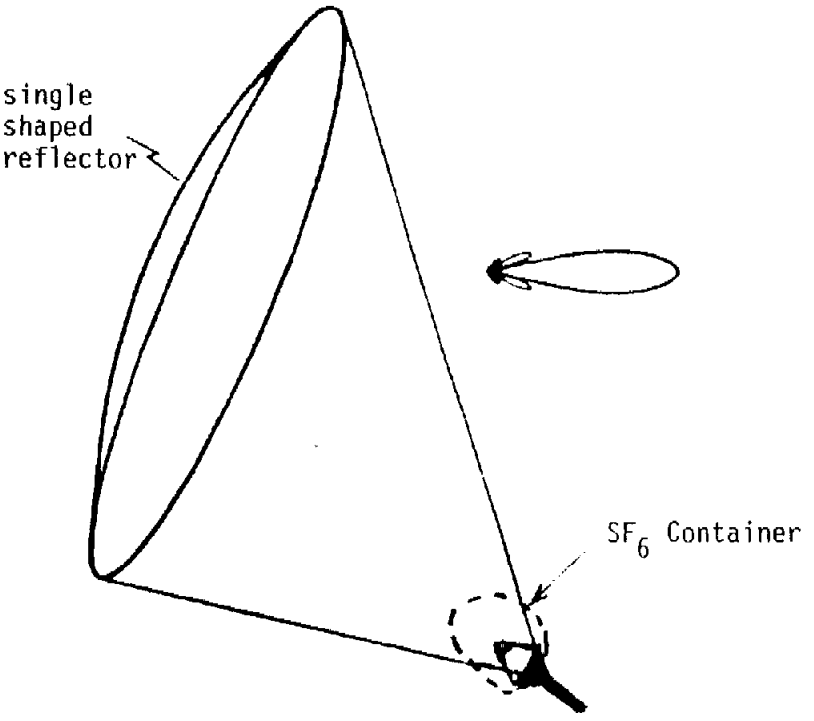

Figure 2. A single reflector system fed by an offset feed horn

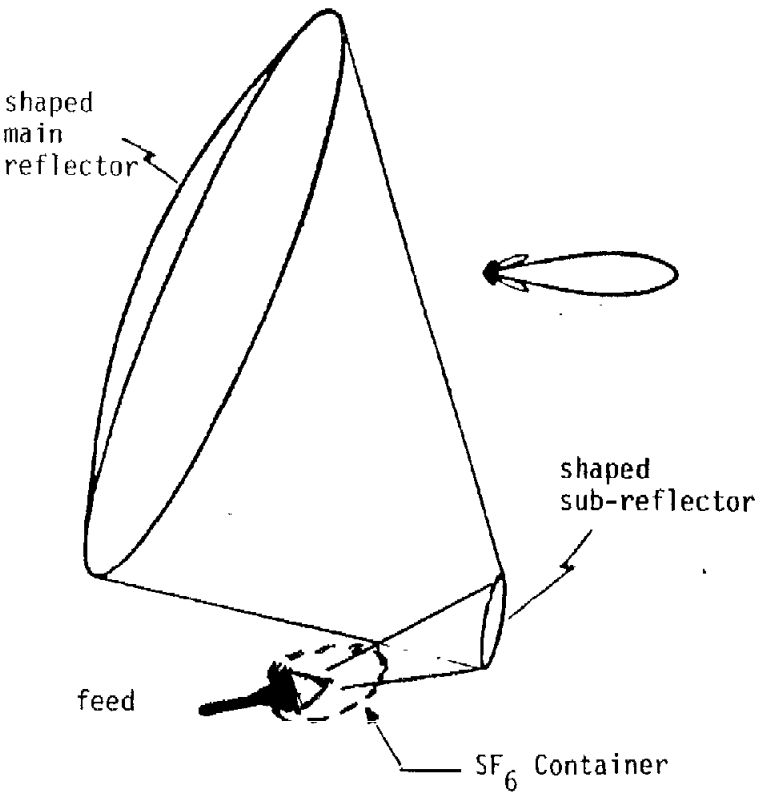

Figure 3. A dual reflector system

In concluding this introductory section, we note that Sections 2 and 3 deal respectively with the waveguides and directional couplers, whereas in section 4 the feed horn and the dielectric interfaces are discussed. Sections 5 and 6 consider the single and the dual reflector systems. Canonical examples of far fields, power and energy densities are estimated as a function of distance, in Section 7. The note is concluded with a summarizing Section 8, followed by a list of references.

2. Rectangular Waveguides

Recall that WR-975 and WR-340 were chosen in [1] for dominant $H_{1,0}$ mode propagation at frequencies of 1 GHz and 3 GHz. The choices were governed by optimizing the power handling capabilities. One would like to choose a waveguide with the largest cross sectional dimensions and operate it at a frequency below the cut off value of the first higher order mode (i.e., $H_{0,1}$ or $H_{2,0}$ modes which both have the same cut off value).

For the canonical examples in this note, we have chosen average power levels P_{avg} of 3 GW and 10 GW at 1 GHz. The average power levels chosen are 1 GW and 3 GW at the higher frequency of 3 GHz. The expression for P_{avg} in a waveguide propagating a $H_{1,0}$ mode is given by [1]

$$P_{avg} = \frac{E_0^2}{2Z_0} \frac{ab}{2} \left[1 - \left[\frac{\lambda}{2a}\right]^2\right]^{1/2} = p_{avg} \left[\frac{ab}{2}\right] \tag{2.1}$$

where

$E_0 \equiv$ peak electric field in the waveguide

$Z_0 \equiv$ characteristic impedance of free space

$a \equiv$ inside larger dimension of the waveguide

$b \equiv$ inside smaller dimension of the waveguide

$\lambda \equiv$ operating wavelength

The power density p_{avg} in the waveguide and the peak power P_{peak} are respectively given by

$$p_{avg} = 2P_{avg}/(a\,b) = \frac{1}{2}\left[E_0^2/Z_{1,0}\right] \tag{2.2}$$

$$P_{peak} = 2P_{avg} \tag{2.3}$$

and the peak electric field in the waveguide is

$$E_{peak} = E_0 = \sqrt{2p_{avg}Z_{1,0}} \tag{2.4}$$

where

$$Z_{1,0} = Z_0\left[1-\left[\frac{\lambda}{2a}\right]^2\right]^{-1/2} \tag{2.5}$$

Figure 4 shows the rectangular waveguide where the inside dimensions are denoted by a and b. The electric or the E-wall and the magnetic or the H-wall are also identified in this figure. This has relevance in the next section where we discuss the directional coupler. In table 1, we list the relevant waveguide parameters at both frequencies of 1 and 3 GHz. Also included in table 1 are the power densities (p_{avg}) and the peak electric fields in the waveguide at the assumed power levels. Few comments about these assumed power levels are in order. Firstly, such power levels and power densities appear to be practically realizable from the HPM sources in a single waveguide [3] by proper choice of waveguide which maximizes the power handling capabilities. Secondly, the associated peak electric fields call for hard vacuum in the waveguide and are also well below the field levels needed for field emission from the inside walls of the waveguides into the vacuum. Field emission occurs in the presence of electric fields of the order of GV/m, the precise field values being governed by frequency, pulse duration and the surface conditions. Field emission is defined as the emission of electrons from the surface of a condensed phase into another phase,

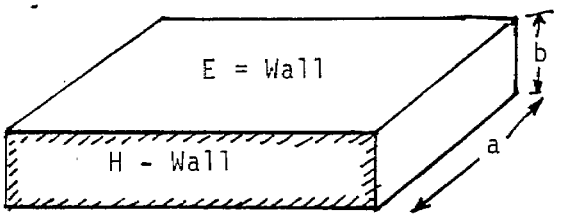

Figure 4. Rectangular waveguide of inside dimensions a and b.

Parameter	f = 1 GHz			f = 3 GHz		
Wavelength λ	0.3 m			0.1 m		
Waveguide	WR 975			WR 340		
Dimensions	a = 247.65 mm b = 123.83 mm			a = 86.36 mm b = 43.18 mm		
$\lambda_c(H_{1,0})$	0.4953 m			0.1727 m		
$f_c(H_{1,0})$	605.69 MHz			1.737 GHz		
$f_c(H_{0,1}) = f_c(H_{2,0})$	1.2114 GHz			3.474 GHz		
$Z_{1,0}$	473.8 Ohms			462.4 Ohms		
	P_{avg} GW	p_{avg} GW/m^2	E_{peak} MV/m	P_{avg} GW	p_{avg} GW/m^2	E_{peak} MV/m
	3	196	13.63	1	536	22.36
	10	652	24.88	3	1608	38.73

Table 1. Rectangular waveguide parameters at the two frequencies and the two power levels (assumed).

usually a vacuum under the influence of high electrostatic fields. In the present context, we are concerned with emission of electrons from the metallic surfaces of the waveguides into the vacuum. The surface potential configuration and the surface condition itself affects the field emission profoundly, in addition to frequency pulse duration etc. So,in practical waveguides, the field emission could start at levels lower than a GV/m. Field ionization is not a factor, since this phenomenon occurs at fields well above those required for field emission. Field emission then is the limiting factor in theory and the peak field numbers we have in table 1 should pose no problem, if suitable vacuum conditions are attained.

3. Directional Couplers

I is desirable to monitor the power which is being transferred through the waveguide, from the HPM source to the antenna system. This monitoring should be accomplished by a simple device which employs some means of coupling a fractional power out of the waveguide. In addition, it is also useful to monitor the reflected power from the antenna back to the HPM source. Bidirectional couplers of various types have been designed and used at low power levels. However, not all of the readily available designs apply in the context of HPM application.

We may consider the field distribution of the dominant $H_{1,0}$ mode in a rectangular waveguide [4] as illustrated in figure 5. The electric field for the dominant mode is given by

$$E_y = E_0 \sin(\pi x/a) \tag{3.1}$$

which is seen to vanish on the magnetic or H-walls at x = 0 and x = a. Consequently, the H-walls are electric charge free and hence in the context of HPM applications, directional couplers that couple through the H-walls are preferable.

A bidirectional coupler suitable for HPM application is illustrated in figure 6. As seen in this figure, a series of small holes in the H-wall of the main waveguide couples power to the bent waveguides. These waveguides are then connected to non-reflecting detector systems to independently monitor both the forward and the reflected powers. A 60 to 80 dB coupler is required to monitor the forward power. Typically, one may have 2 holes in the H-wall that are separated by $\lambda_g/4$ which is efficient at a single frequency. A series of holes may be employed to provide for some bandwidth for the

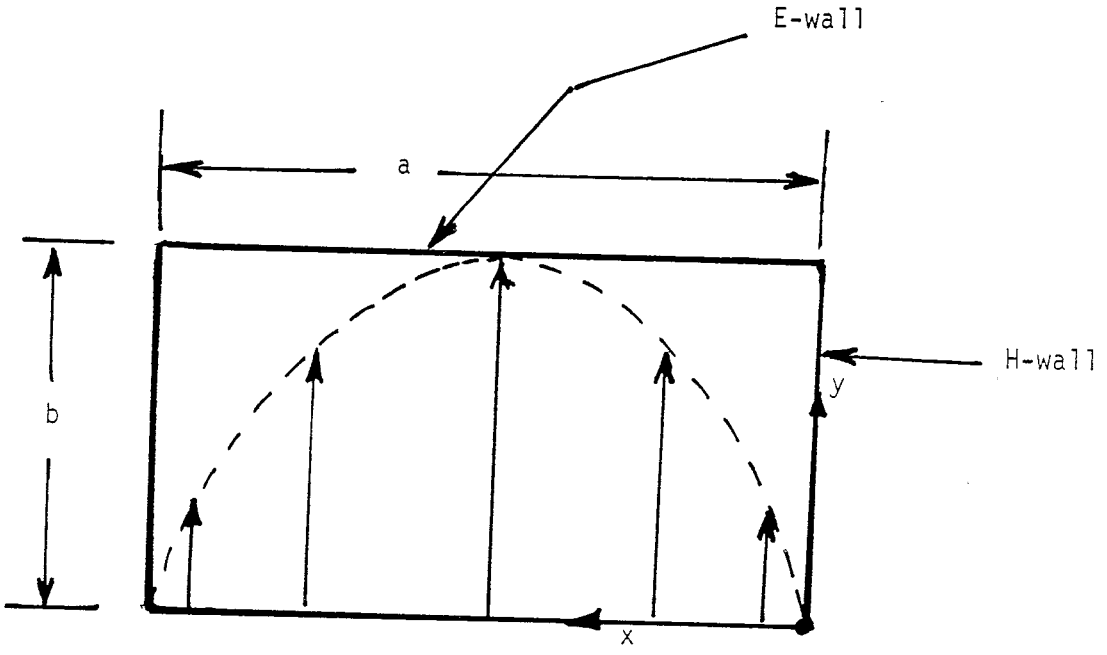

Figure 5. Cross section of a rectangular waveguide showing the $H_{1,0}$ mode electric field.

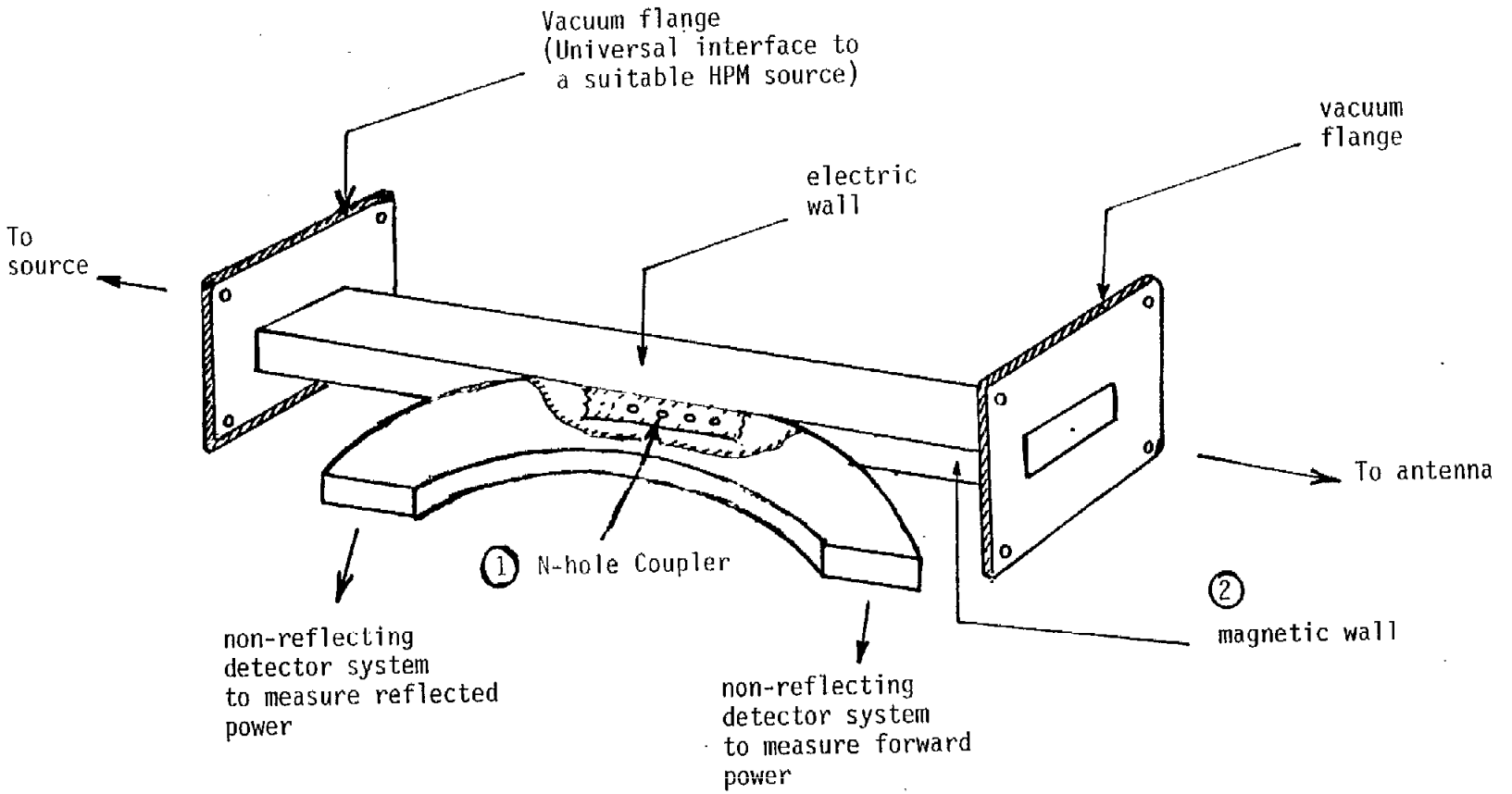

Figure 6. Magnetic wall bidirectional coupler (60-80 dB)

Notes

① several holes in the magnetic wall will provide some bandwidth

② the electric field and electric charge vanishess on the magnetic wall

bidirectional coupler. The performance features of these couplers may be optimized at low power level tests. It may also be noted that directional couplers for monitoring only the forward power can also be built if needed. The modification to figure 6 would then consist of providing for a matched load in the port carrying the reflected power and, maybe even avoid the bending of the waveguide that carries a fraction of the reflected power.

4. Single Horn Feed

The reflector antenna systems under consideration here are fed by a single horn, which is connected to a vacuum flange to the waveguide run starting at the end of the directional coupler. The single feed horn is illustrated in figure 7. The pyramidal electromagnetic horn of figure 7 is for illustrative purposes only. What is of interest here is to discuss the design aspects of such a horn in the HPM context. At low power levels, the theory of design and performance of single horns are well known.

In the HPM application, where the power levels are in the GW range, the waveguide and the horn are evacuated. Horn aperture size is such that the power density and the peak electric field at the mouth of the horn enable a transition from vacuum to 1 atmosphere SF_6 gas. Nominally, this means the peak electric field at the horn aperture be below 3 MV/m to avoid excessive electrical stresses causing a breakdown. If the horn aperture has dimensions a′ (width, larger than the height) and b′ (height) corresponding to a and b of the waveguide, the peak electric field at the aperture is estimated by

$$E_{peak} \text{ (at the horn)} = E_{peak} \text{ (waveguide)} \times \sqrt{\frac{ab}{a'b'}} \qquad (4.1)$$

As an example, for a pyramidal horn with equal E and H plane angles, i.e., $(a/a') = (b/b')$, we have

$$E_{peak}\text{(at the horn)} = E_{peak}\text{(waveguide)} \times (b/b') \qquad (4.2)$$

As an example from table 1, at f = 1 GHz and P_{avg} = 3 GW, the peak electric field in the waveguide was found to be 13.63 MV/m, which means (b/b′) should be about 0.22

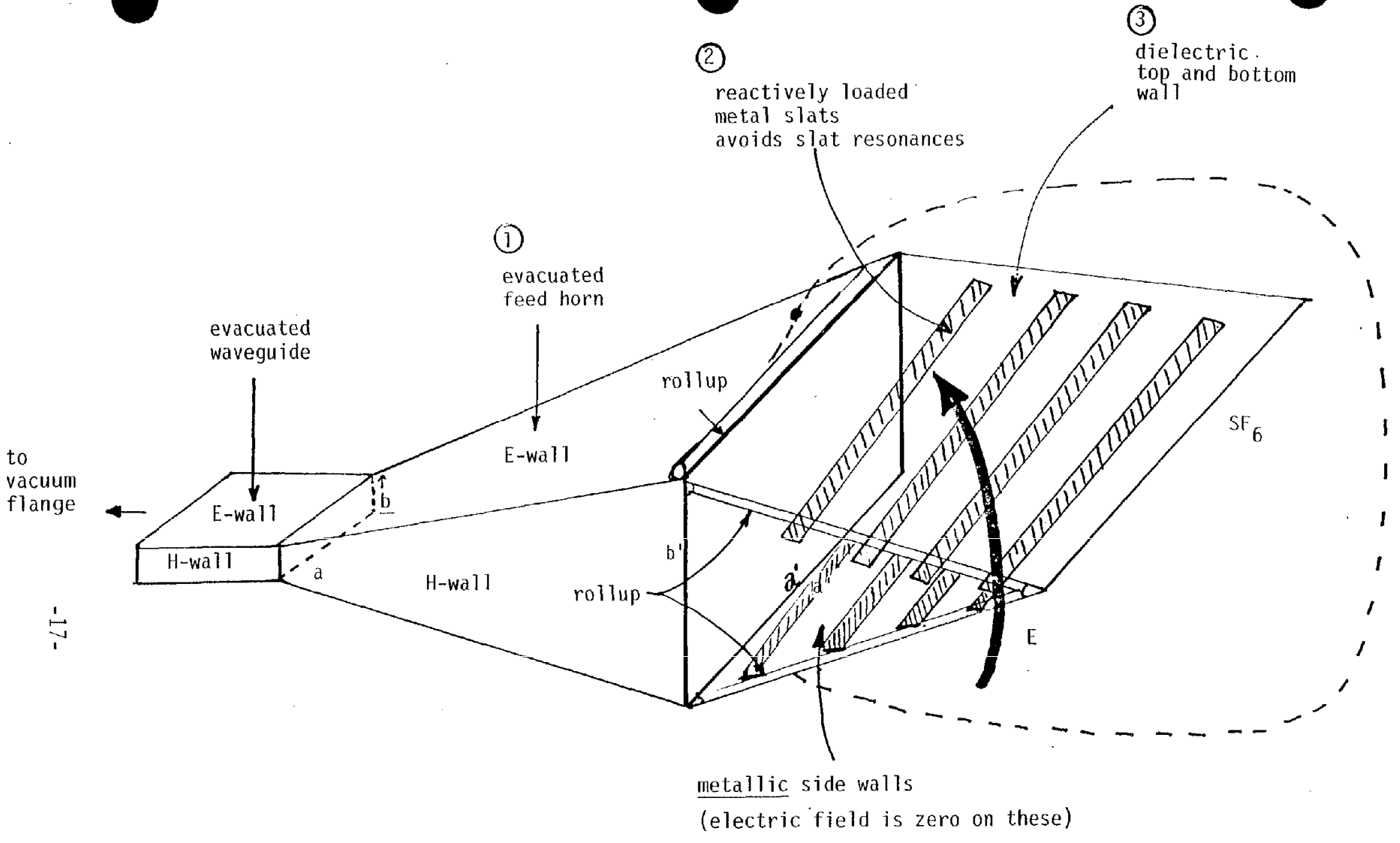

Figure 7. Some details of the proposed feed horn

Note

① the feed horn (e.g., pyramidal, diagonal, square etc.)

② metal slats designed to support the pressure difference

③ electric field is not parallel to the dielectric interface, helps in avoiding tracking

in order to keep the electric field below 3 MV/m at the mouth of the horn, where we have an interface between the vacuum and SF_6 at 1 atmospheric pressure. Consequently, the minimum dimension of b′ is 4.55 b = 0.56 m for b = 12.383 cm. In terms of wavelengths, b′ at the horn aperture is 1.87 λ, at the minimum. The basic requirement is that (b′/b) or the horn aperture height should be large enough to permit the interface from vacuum to SF_6 at the mouth of the horn. The dielectric interace can take many forms as discussed in [5], but the configuration of the interface sketched in figure 7 offers many advantages for HPM application. First of all, note that the H-walls of the electromagnetic horn can continue to be metallic (if need be) beyond the horn aperture, since the electric field vanishes on these surfaces. The top and bottom ''E-walls'' are extended beyond the horn aperture as dielectric sheets that are flaring out. Metallic slats can be introduced, fastened to the side walls. The metallic slots are orthogonal to the direction of the electric field. These slats provide mechanical stability and counteract the gas pressure (1 atmosphere SF_6) on the dielectric interface. It is also observed that the total electric field in this region is *not* parallel to the dielectric interface which helps in avoiding tracking etc. One may want to reactively load the metallic slats (e.g., series inductance in the slats) to modify the resonances of the slats themselves. Outside the interface, the medium is SF_6 gas at a pressure of 1 atmosphere contained in a polyethylene bag. This SF_6 container is large enough so that anywhere outside of this container, the peak electric field is of the order of 1 MV/m or less and the medium outside is air. Yet another feature useful in HPM application is that all of the metallic edges at the mouth of the horn may be rolled-up in a cylindrical or conical roll to reduce field enhancement.

It is important to note that the HPM radiating system is designed to maximize the electric field at a distance, under certain conditions and constraints. This is not an antenna for radio-astronomy or a part of a high precision communication system. HPM brings into play certain design complexities, however the antenna requirements are not the same as in a satellite communication link.

The precise size and shape of the horn aperture has to take into consideration that the radiation pattern of the horn should match the required illumination of the reflector or the subreflector [6]. In other words, the reflector efficiency plays a role in the design of the horn aperture, in terms of filling the reflector or the subreflector and minimizing the spill over energy. We have seen above that the horn aperture height (b′ in figure 7) should have a certain minimum value to avoid electrical breakdown, for a given P_{avg} power carried out of the source. Table 2 lists the values of minimum b′ for the different cases considered here.

f = 1 GHz

	waveguide					horn
P_{avg} GW	E_{peak} MV/m	b cm	b/λ	minimum b' cm	minimum b'/λ	E_{peak} MV/m
3	13.63	12.383	0.41	56.3	1.87	3
10	24.88	12.383	0.41	102.7	3.42	3

f = 3 GHz

	waveguide					horn
P_{avg} GW	E_{peak} MV/m	b cm	b/λ	minimum b' cm	minimum b'/λ	E_{peak} MV/m
1	22.36	4.318	0.43	32.2	3.22	3
3	38.73	4.318	0.43	55.75	5.57	3

TABLE 2. Minimum values of the height b' of the horn aperture in order to achieve a peak electric field of 3 MV/m at the horn aperture (vacuum/1 atm. SF_6 interface location)

5. Offset Parabolic Reflector

Efficient computational methods are available [7] for obtaining far-field patterns of offset reflectors that are illuminated by pyramidal horns. It is observed that the performance characteristics of reflector antennas cannot be evaluated without a proper description of the feed element. This is especially true in the HPM context, since we require the feed horn to have certain minimum dimensions. So the design of the feed element and the reflector antenna should be integrated, in evaluating the overall performance.

One could also distinguish between ''low-field'' and ''high-field'' situations, as illustrated in figures 8 and 9. In the low-field situation of figure 8, the peak electric field is about 1 MV/m at point P in front of the feed horn and everywhere outside the SF_6 container, the peak electric field is constrained to be under 1 MV/m. In particular the peak electric field incident at the reflector, will be much below 1 MV/m. Recall that the far field is directly proportional to the field at the reflector.

A second choice is the ''high-field'' case of figure 9. In this case, we have a situation in which the peak electric field incident at the reflector antenna is about 1 MV/m, leading to the maximization of the field at a distance. One of the primary differences is of course, the design of the dielectric interface and the SF_6 container are different from the low-field case. In the high-field case, the large single reflector is contained in the SF_6 environment. Peak fields as a function of distance away from the reflector are estimated in the next section, for a set of assumed parameters about the reflector antenna system.

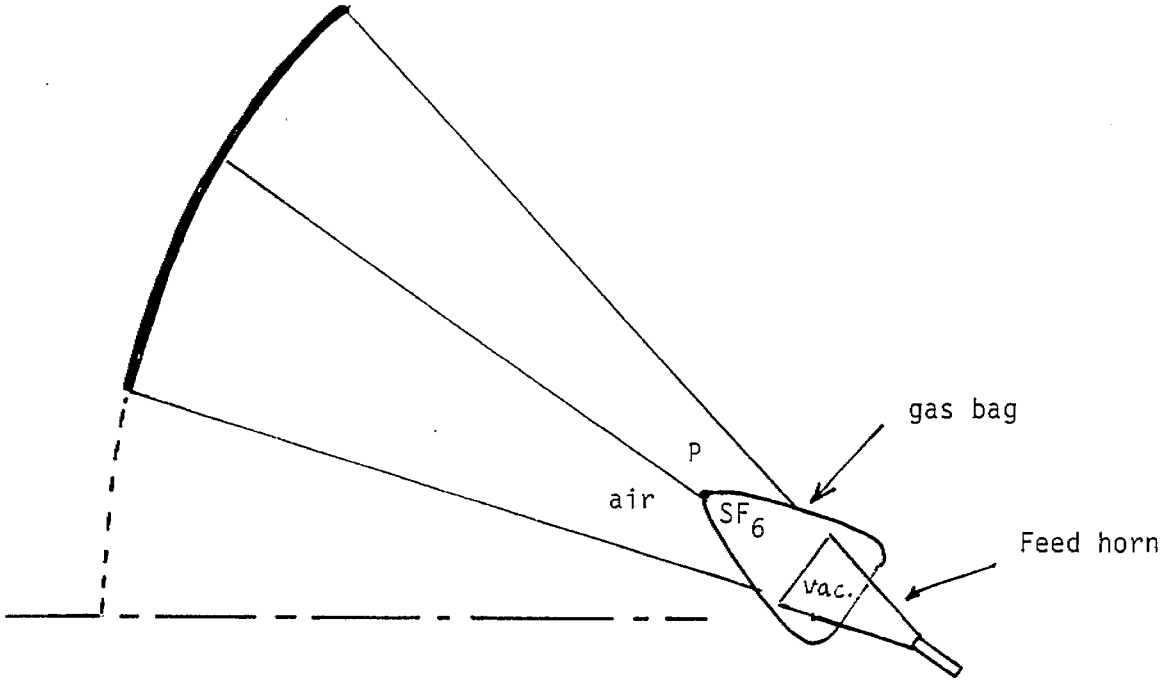

Figure 8. Offset parabolic reflector (low-field at the aperture) with about a 1 MV/m peak electric field at the point P.

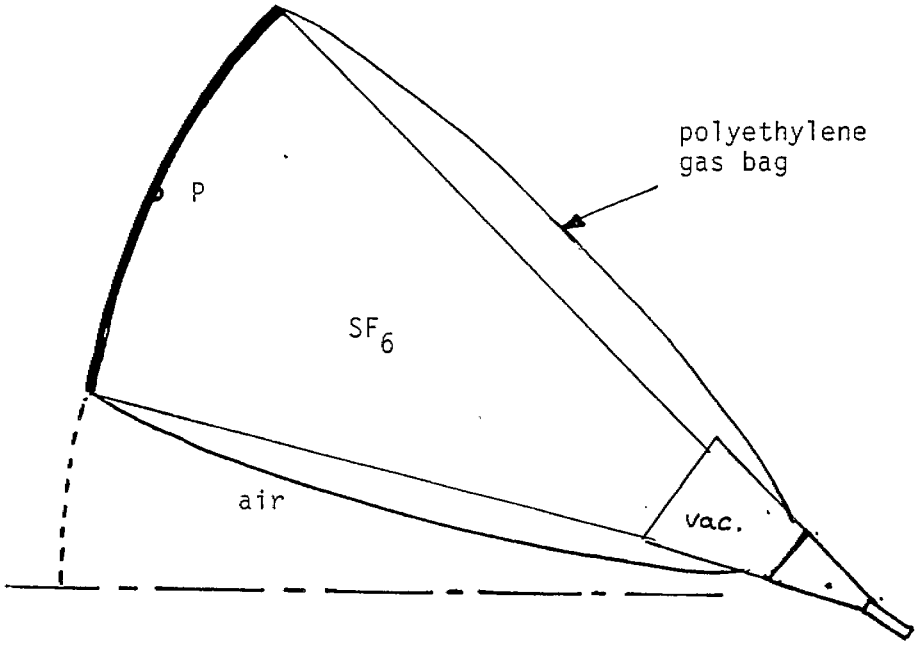

Figure 9. Offset parabolic reflector (high-field at the aperture with about a 1 MV/m peak electric field at the dish.

(Note that the reflector aperture is not necessarily circular since practical considerations may constrain this to a rectangular, elliptical or square shapes)

6. Offset Dual Reflector (Cassegrain)

Both offset and symmetric Cassegrain reflector antennas are used in satellite and ground communication systems [8]. With some modifications, an offset Cassegrain system is well suited for the HPM application. The modifications consist of the hardware required to avoid electrical breakdown in the vicinity of the antenna. In addition the feed horn dimensions at its mouth are also governed by the field levels there. Consequently, the design of the feed and the reflectors (main and sub) have all to be integrated, while meeting all of the requirements due to the high power and field levels.

As in the case of the single reflector system of the previous section, one could distinguish between the ''low-field'' and ''high-field'' situations here, as illustrated in figure 10 and 11. In the low-field situation of figure 10, the peak electric is about 1 MV/m or less at all points outside the SF_6 container. This container is seen to include the subreflector in it. In particular, the peak electric field incident at the main reflector, will be much below 1 MV/m, recalling that the field at a distance is directly proportional to the field at the reflector.

As before, a second choice is the ''high-field'' case of figure 11. In this case, we have a situation in which the peak electric field incident at the main reflector is about 1 MV/m, resulting in the maximization of the field at a distance. In the low-field case, only the subreflector is inside the SF_6 container, whereas in the high-field case, both the main and subreflectors are contained in a SF_6 environment.

The offset Cassegrain provides for beam steering (± 10 beam widths) by moving

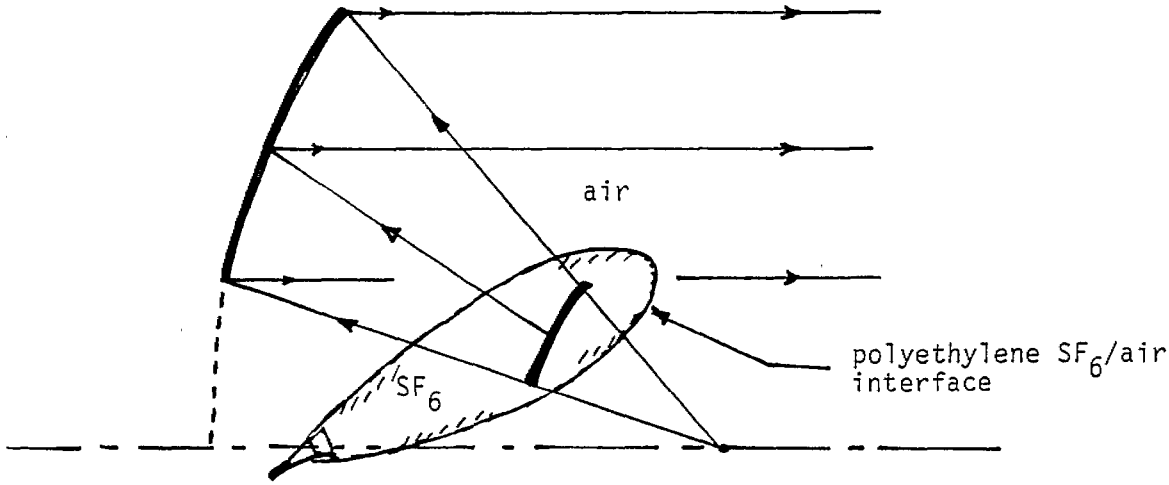

Figure 10. Dual reflector system (low-field at the larger reflector) e.g., offset Cassegrain with about a 1 MV/m peak electric field at the subreflector which is moved inside the gas bag.

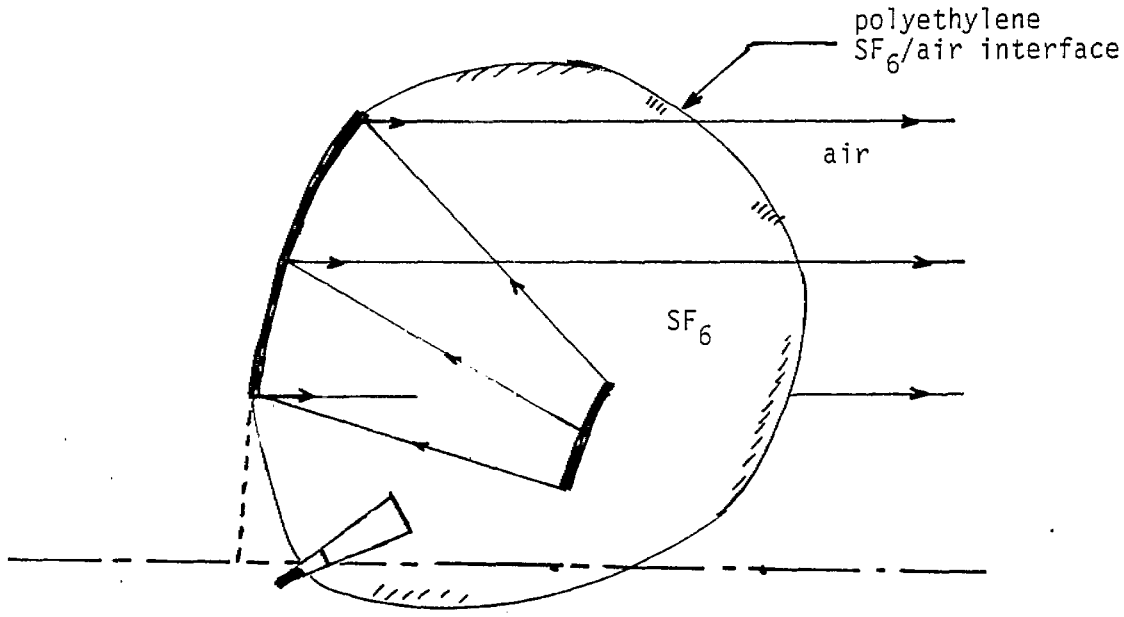

Figure 11. Dual reflector system (high-field at the larger reflector) e.g., offset Cassegrain with about a 1 MV/m peak electric field at the larger reflector and the subreflector moving inside the gas bag.

(Note that the reflector aperture is not necessarily circular since practical considerations may constrain this to a rectangular, sqaure or elliptical shapes)

the subreflector in the SF_6 container. Peak fields as a function of distance away from the reflector can be estimated for a set of Cassegrain reflector antenna design parameters.

In the next section, we consider for example, the offset parabolic reflector antenna of Section 5 and work out a few canonical examples. Calculations such as these can be repeated later for the Cassegrain system. With a single feed and somewhat relaxed constraints on beam steering, the single reflector system (i.e., offset parabolic reflector) is relatively simpler than the dual reflector system.

7. Canonical Examples

We have earlier made assumptions about the frequency and average power levels. The values were:

f = 1 GHz ; $P_{avg} = 3GW$ and 10 GW

f = 3 GHz ; $P_{avg} = 1GW$ and 3 GW

We further assume two values of pulse widths Δt given by

Δt = 100 ns and 1 μs

Next, we need to assume certain values for the area A of the main reflector of Section 5 or 6. We have considered values of 20 m^2, 40 m^2 and 100 m^2, corresponding to dish diameters (if circular) of 5.05 m, 7.14 m and 11.28 m, which are quite practical. For these reflector sizes, the far fields start approximately at a distance $R \geq (2d^2/\lambda)$ where d is the reflector diameter and λ is the operating wavelength. The values of R at the assumed frequency of 1 GHz, for the three reflectors are 170 m, 340 m and 850 m. The values of R at the assumed frequency of 3 GHz for the three reflectors are 510 m, 1.02 km and 2.54 km. The far field estimates will be valid at R values greater than the $(2d^2/\lambda)$ values above.

Consider for example, the offset parabolic reflector antenna of figure 8. Let us assume that the criterion of minimum height b' of the horn aperture from Table 2 is satisfied as noted below:

f = 1 GHz P_{avg} = 3 GW $b' = 2\lambda$

f = 1 GHz P_{avg} = 10 GW b′ = 3.5λ

f = 3 GHz P_{avg} = 1 GW b′ = 3.5λ

f = 3 GHz P_{avg} = 3 GW b′ = 6λ

b′ is the height of the horn aperture and above values satisfy the minimum height criteria required to interface from vacuum to SF_6. Knowing the height b of the waveguide and b′, it is a simple matter to estimate the peak electric field value at the horn aperture, to ensure that it is below 3 MV/m to permit vacuum/SF_6 transition.

Next, one can estimate approximately the field at the reflector by scaling the field in the waveguide by a factor of waveguide height to reflector height. Knowing the field at the reflector, the far field parameters may then be estimated using

$$E_{peak}(\text{far field}) = E_{peak}(\text{reflector}) \left[\frac{A}{R\lambda}\right] V/m$$

$$p_{avg}(\text{far field}) = \left[\frac{E^2_{peak}(\text{far field})}{2Z_0}\right] W/m^2$$

$$\text{energy density} \equiv u = (p_{avg}\,\Delta t) \quad J/m^2$$

recalling that we have assumed two values of Δt to be 100 ns and 1 μs. Tables 3 to 6 contain estimates of far field parameters. The frequency of operation and the average power P_{avg} is held fixed on each of these tables. Three values of A and 2 values of Δt are considered for each set. One can see the peak far field (kV/m) as a function of distance R away from the reflector. The average power density and energy density (for both values of pulse width Δt) are also tabulated. The reflector antenna aperture

TABLE 3. Estimates of far field quantities (f = 1 GHz)

U ≡ microwave energy from the source = {300J at Δt = 100 ns; 3 KJ at Δt = 1 μs}

Waveguide: P_{avg} = 3 GW E_{peak} = 13.63 MV/m

Horn Aperture: height b' = 2λ E_{peak} = 2.81 MV/m

A = 20 m^2
d = 5.05 m
E_p(refl) = 335 KV/m

R Km	$\frac{A}{R\lambda}$	E_{peak} KV/m	P_{avg} KW/m^2	u(J/m^2) Δt 100 ns	u(J/m^2) Δt 1 μs
0.2	0.33	111	16337	1.63	16.3
1	0.07	23	702	7.0×10^{-2}	0.7
10	0.007	2.3	7.02	7.0×10^{-4}	7.0×10^{-3}
50	0.001	0.45	0.28	2.8×10^{-5}	2.8×10^{-4}
100	0.0007	0.23	0.07	7.0×10^{-6}	7.0×10^{-5}

A = 40 m^2
d = 7.14 m
E_p(refl) = 236 KV/m

R Km	$\frac{A}{R\lambda}$	E_{peak} KV/m	P_{avg} KW/m^2	u(J/m^2) Δt 100 ns	u(J/m^2) Δt 1 μs
0.5	0.27	63.72	5384	0.54	5.4
1	0.13	30.68	1248	0.12	1.2
10	0.013	3.07	12.5	1.2×10^{-3}	1.2×10^{-2}
50	0.003	0.71	0.67	6.7×10^{-5}	6.7×10^{-4}
100	0.0013	0.31	0.13	1.3×10^{-5}	1.3×10^{-4}
200	0.0007	0.16	0.03	3.0×10^{-6}	3.0×10^{-5}

A = 100 m^2
d = 11.28 m
E_p(refl) = 150 KV/m

R Km	$\frac{A}{R\lambda}$	E_{peak} KV/m	P_{avg} KW/m^2	u(J/m^2) Δt 100 ns	u(J/m^2) Δt 1 μs
1	0.333	50	3315	0.33	3.3
10	0.033	5	33.15	3.3×10^{-3}	3.3×10^{-2}
50	0.007	1	1.33	1.3×10^{-4}	1.3×10^{-3}
100	0.003	0.5	0.33	3.3×10^{-5}	3.3×10^{-4}
200	0.0017	0.25	0.08	8.0×10^{-6}	8.0×10^{-5}
500	0.0007	0.1	0.01	1.0×10^{-6}	1.0×10^{-5}

TABLE 4. Estimates of far field quantities (f = 1 GHz)

Waveguide: P_{avg} = 10 GW E_{peak} = 24.88 MV/m

Horn Aperture: height b' = 3.5 λ E_{peak} = 2.93 MV/m

U = microwave energy from the source

$= \begin{cases} 1\text{KJ at } \Delta t = 100 \text{ ns} \\ 10\text{KJ at } \Delta t = 1\ \mu s \end{cases}$

A = 20 m^2
d = 5.05 m
E_p(refl) = 611 KV/m

Km	$\frac{A}{R\lambda}$	E_{peak} KV/m	P_{avg} KW/m^2	u(J/m^2) Δt 100 ns	u(J/m^2) Δt 1 μs
0.2	0.33	202.6	54,428	5.44	54.4
1	0.07	42.1	2,350	0.23	2.3
10	0.007	4.21	23.50	2.3×10^{-3}	2.3×10^{-2}
50	0.001	0.82	0.89	8.9×10^{-5}	8.9×10^{-4}
100	0.0007	0.42	0.23	2.3×10^{-5}	2.3×10^{-4}
200	0.0003	0.20	0.05	5×10^{-6}	5×10^{-5}

A = 40 m^2
d = 7.14 m
E_p(refl) = 431 KV/m

R Km	$\frac{A}{R\lambda}$	E_{peak} KV/m	P_{avg} KW/m^2	u(J/m^2) Δt 100 ns	u(J/m^2) Δt 1 μs
0.5	0.27	116.6	18,027	1.80	18.0
1	0.13	56.1	4,173	0.42	4.2
10	0.013	5.62	41.8	4.2×10^{-3}	4.2×10^{-2}
50	0.003	1.30	2.24	2.2×10^{-4}	2.2×10^{-3}
100	0.0013	0.57	0.43	4.3×10^{-5}	4.3×10^{-4}
200	0.0007	0.29	0.11	1.1×10^{-5}	1.1×10^{-4}
500	0.0003	0.11	0.02	2×10^{-6}	2×10^{-5}

A = 100 m^2
d = 11.28 m
E_p(refl) = 274 KV/m

R KM	$\frac{A}{R\lambda}$	E_{peak} KV/m	u(J/m^2) Δt 100 ns	u(J/m^2) Δt 1 μs
1	0.333	91.5	1.11	11.1
10	0.033	9.15	1.1×10^{-2}	0.11
50	0.007	1.83	4.4×10^{-4}	4.4×10^{-3}
100	0.003	0.92	1.12×10^{-4}	1.12×10^{-3}
200	0.0017	0.46	2.8×10^{-5}	2.8×10^{-4}
500	0.0007	0.18	4.0×10^{-6}	4.0×10^{-5}

TABLE 5. Estimates of far field quantities (f = 3GHz)

U ≡ microwave energy from the source

= {100J at Δt = 100 ns; 1 KJ at Δt = 1 μs}

Waveguide: P_{avg} = 1 GW E_{peak} = 22.36 MV/m

Horn Aperture: height b' = 3.5 λ E_{peak} = 2.76 MV/m

A = 20 m^2
d = 5.05 m
E_p(refl) = 190 KV/m

R Km	$\frac{A}{R\lambda}$	E_{peak} KV/m	P_{avg} KW/m^2	u(J/m^2) Δt 100 ns	u(J/m^2) Δt 1 μs
0.5	0.40	76	7,659	0.77	7.7
1	0.20	38	1,914	0.19	1.9
5	0.04	7.6	76.6	7.6×10^{-3}	7.6×10^{-2}
10	0.02	3.8	1.91	1.9×10^{-4}	1.9×10^{-3}
50	0.004	0.76	0.76	7.6×10^{-5}	7.6×10^{-4}
100	0.002	0.38	0.19	1.9×10^{-5}	1.9×10^{-4}

A = 40 m^2
d = 7.14 m
E_p(refl) = 140 KV/m

R Km	$\frac{A}{R\lambda}$	E_{peak} KV/m	P_{avg} KW/m^2	u(J/m^2) Δt 100 ns	u(J/m^2) Δt 1 μs
1	0.4	56	4,158	0.42	4.2
2	0.2	28	1,040	0.1	1.04
5	0.08	11.2	166.3	1.6×10^{-2}	0.16
10	0.04	5.6	41.6	4.1×10^{-3}	4.1×10^{-2}
50	0.008	1.12	1.66	1.6×10^{-4}	1.6×10^{-3}
100	0.004	0.56	0.41	4.1×10^{-5}	4.1×10^{-4}
200	0.002	0.28	0.104	1.0×10^{-5}	1.0×10^{-4}

A = 100 m^2
d = 11.28 m
E_p(refl) = 90 KV/m

Km	$\frac{A}{R\lambda}$	E_{peak} KV/m	P_{avg} KW/m^2	u(J/m^2) Δt 100 ns	u(J/m^2) Δt 1 μs
2.5	0.4	36	1,718	0.17	1.7
5	0.2	18	430	0.04	0.4
10	0.1	9	107	1.0×10^{-2}	0.1
50	0.02	1.8	4.3	4.3×10^{-4}	4.3×10^{-3}
100	0.01	0.9	0.82	8.2×10^{-5}	8.2×10^{-4}
500	0.002	0.[illegible]	0.04	4×10^{-6}	4×10^{-5}

TABLE 6. Estimates of far field quantities (f = 3 G

Waveguide: P_{avg} = 3 GW E_{peak} = 38.73 MV/m U = microwave energy from the source

Horn Aperture: height b' = 6 λ E_{peak} = 2.79 MV/m {300J at Δt = 100 ns; {3 KJ at Δt = 1 μs

A = 20 m^2
d = 5.05 m
E_p(refl) = 331 KV/m

R Km	$\frac{A}{R\lambda}$	E_{peak} KV/m	p_{avg} KW/m^2	u(J/m^2) Δt 100 ns	u(J/m^2) Δt 1 μs
0.5	0.4	132.4	23,244	2.32	23.2
1	0.2	66.2	5,811	0.58	5.8
2	0.1	33.1	1,453	0.14	1.4
5	0.04	13.2	231	0.02	0.2
10	0.02	6.62	58	5.8×10^{-3}	5.8×10^{-2}
50	0.004	1.32	2.31	2.3×10^{-4}	2.3×10^{-3}
100	0.002	0.66	0.58	5.8×10^{-5}	5.8×10^{-4}
200	0.001	0.33	0.14	1.4×10^{-5}	1.4×10^{-4}

A = 40 m^2
d = 7.14 m
E_p(refl) = 234 KV/m

R Km	$\frac{A}{R\lambda}$	E_{peak} KV/m	p_{avg} KW/m^2	u(J/m^2) Δt 100 ns	u(J/m^2) Δt 1 μs
1	0.4	93.6	11,617	1.16	11.6
2	0.2	46.8	2,904	0.29	2.9
5	0.08	18.7	464	0.04	0.4
10	0.04	9.36	116	0.01	1.0
50	0.008	1.87	4.6	4.6×10^{-4}	4.6×10^{-3}
100	0.004	0.93	1.14	1.14×10^{-4}	1.14×10^{-3}
500	0.001	0.18	0.04	4.0×10^{-6}	4.0×10^{-5}

A = 100 m^2
d = 11.28 m
E_p(refl) = 148 KV/m

R KM	$\frac{A}{R\lambda}$	E_{peak} KV/m	p_{avg} KW/m^2	u(J/m^2) Δt 100 ns	u(J/m^2) Δt 1 μs
2.5	0.4	59.2	4647	0.46	4.6
5	0.2	29.6	1161	0.11	1.1
10	0.1	14.8	290	0.03	0.3
50	0.02	2.96	11.6	1.1×10^{-3}	1.1×10^{-2}
100	0.01	1.48	2.9	2.9×10^{-4}	2.9×10^{-3}
500	0.002	0.29	0.11	1.1×10^{-5}	1.1×10^{-4}

areas (A = 20 m^2, 40 m^2 and 100 m^2) are also used in determining the diameter of the reflector (5.05 m, 7.14 m and 11.28 m). Once again, these parameters are tabulated for illustrative purposes. Actual sizes and shapes of the feed horn and the reflector need to be determined with due regard to the proper illumination of the reflector. The parameters in the tables 3-6, help in setting a framework for the actual design of the radiating systems. The tables merely point out the practical constraints on sizes and estimate what is achievable in the far field.

8. Summary

In this note, we have considered some canonical examples of HPM radiation systems, under the assumption of a single evacuated rectangular waveguide being employed to extract the power from the source. Two frequencies (1 GHz and 3 GHz) are considered, as well as two power levels at each frequency. Two values of pulse widths (Δt = 100 ns and 1 μs) and three values of the radiating aperture area (A = 20 m^2, 40 m^2 and 100 m^2) are also considered. For each of these source/antenna configurations, far field parameters such as peak electric field, average power densities and energy densities are estimated. These estimates are obtained to set a framework and ranges of parametric values for future designs of specific antenna systems.

An important aspect of the radiation system, namely the horn feed optimization leading to best illuminate the reflector is not considered yet. Given the range of parametric values of such quantities as P_{avg}, A, f, Δt etc., specific designs can now be addressed in future reports.

Important future work needed may be listed as follows

1) measurement on allowable fields in vacuum including surface conditions and pulse widths

2) horn feed pattern optimization (shaping) leading to best filling of the reflector(s)

3) rectangular/elliptical reflectors versus square or circular to obtain both polarizations.

s

Reference

[1] D. V. Giri, "Preliminary Considerations for High-Power Microwave (HPM) Radiating Systems," Circuit and Electromagnetic System Design Note 40, 28 December 1990.

[2] D. W. Duan and Y. Rahmat-Samii, "Antennas for High-Power Microwave Applications--Part I," UCLA Report No. ENG-90-21, US Army Research Grant DAAL02-89-K-0129, September 10, 1990.

[3] V. L. Grantstein and I. Alexeff, Editors, *High-Power Microwave Sources,* Artech House, Norwood, MA, 1987, Chapter 10, pp. 351-395.

[4] N. Marcuvitz, editor, *Waveguide Handbook,* Dover 1965.

[5] C. E. Baum, "Some Features of Waveguide/Horn Design," Sensor and Simulation Note 314, 18 November 1988.

[6] C. E. Baum, "Focussed Aperture Antennas," Sensor and Simulation Note 306, 19 May 1987.

[7] J. Huang, Y. Rahmat-Samii and K. Woo, "A GTD Study of Pyramidal Horns for Offset Reflector Antenna Applications," *IEEE Trans. on Antennas and Propagation,* Vol. AP-31, No. 2, March 1983, pp. 305-309.

[8] Y, Rahmat-Samii, "Subreflector Extension for Improved Efficiencies in Cassegrain Antennas--GTD/PO Analysis," *IEEE Trans. on Antennas and Propagation,* Vol. AP-34, No. 10, October 1986, pp. 1266-1269.